Influence of age on masonry bond strength and mortar microstructure[1]

Heber Sugo, Adrian W. Page, and Stephen Lawrence

Abstract: The effect of age on bond strength and mortar microstructure was investigated as part of an ongoing masonry bond strength research program at The University of Newcastle. Previous work has shown that both strength losses and strength gains occur with age. The potential loss of bond strength with time has structural implications as the design of masonry using the Australian masonry standard AS 3700–2001 is based on the 7 d bond strength. In this investigation, a single mortar-and-unit combination (dry pressed clay and 1:1:6 mortar) cured under ambient laboratory conditions was studied. Bond strength was determined at ages ranging from 3 to 365 d using a small-scale uniaxial tension test. Maximum bond strength was observed to occur at 180 d with strength minima occurring at 90 and 365 d. Scanning electron microscopy and X-ray diffraction techniques were used to further identify the mortar constituents and hydration levels. Changes in the density of the paste microstructure were observed up to 28 d, which correlated with the initial increase in bond strength. No other microstructural change to account for the strength variations between 28 and 365 d could be observed using these techniques.

Key words: brick–mortar bond, bond mechanism, bond strength, mortar microstructure, age.

Résumé : L'effet du vieillissement sur la résistance du joint de maçonnerie et la microstructure du mortier a été examiné dans le cadre d'un programme permanent de recherche sur la résistance du joint de maçonnerie à l'Université de Newcastle. Les travaux antérieurs ont démontré que les pertes et les gains de résistance survenaient avec le vieillissement. La perte potentielle de résistance du joint de maçonnerie dans le temps présente des implications structurales puisque les calculs de maçonnerie utilisant le norme Australien AS 3700–2001 sont basés sur une résistance du joint de maçonnerie après sept jours. Dans la présente étude, une seule combinaison mortier/unité (argile pressée à sec et mortier 1 : 1 : 6) mûrie sous les conditions ambiantes du laboratoire a été examinée. La résistance du joint de maçonnerie a été déterminée à des âges variant de 3 à 365 jours par un essai de traction uniaxiale à petite échelle. La résistance maximale du joint de maçonnerie a été observée après 180 jours et la résistance minimale a été remarquée à 90 et à 365 jours. La microscopie électronique à balayage et les techniques de diffractions des rayons-X ont été utilisées pour identifier plus à fond les composantes du mortier et les niveaux d'hydratation. Les changements dans la densité de la microstructure de la pâte ont été observés jusqu'au 28e jour, ce qui correspond à l'augmentation initiale de la résistance du joint de maçonnerie. Aucun autre changement de la microstructure n'a été observé au moyen de ces techniques pour justifier les variations de résistance entre 28 et 365 jours.

Mots-clés : lien brique–mortier, mécanisme d'adhérence, résistance du joint de maçonnerie, microstructure du mortier, âge.

[Traduit par la Rédaction]

Introduction

The primary functions of hardened mortar in unreinforced masonry are to provide a durable and weather-tight joint with adequate bond strength. Bond strength is necessary for the effective performance of the masonry under imposed shear loads and particularly out-of-plane loads. The Australian masonry standard AS3700 (Standards Australia 2001) specifies the 7 d bond strength to be used in the design of masonry structures. While any further increases in strength with time would provide an added safety margin, any fall in strength below the 7 d value may potentially reduce the integrity of the structure.

The initiation of the bond development phase takes place with the assembly of fresh mortar and masonry units. The subsequent setting of the cement compounds is preceded by the absorption of mortar fluids into the masonry unit and the resultant transport of mortar fines in the joint to the mortar–brick interface (Sugo et al. 1997; Sugo 2000). The development of significant flexural strength in contemporary mortars is due to the hydration of the Portland cement component. Therefore, it is likely that the factors that influence the rate of cement hydration also directly influence the development of flexural strength in masonry. It could also be expected that continued hydration over longer periods of time would further increase the bond strength. However, the research cited in this paper highlights that a

Received 7 June 2007. Revision accepted 29 October 2007. Published on the NRC Research Press Web site at cjce.nrc.ca on 7 December 2007

H. Sugo,[2] A.W. Page, and S. Lawrence. School of Engineering, Faculty of Engineering and Built Environment, The University of Newcastle, University Drive, Callaghan N.S.W. 2308, Australia.

Written discussion of this article is welcomed and will be received by the Editor until 31 March 2008.

[1]This article is one of a selection of papers published in this Special Issue on Masonry.

[2]Corresponding author (e-mail: Heber.Sugo@newcastle.edu.au).

continuous increase in strength is not always observed, with both strength losses and gains occurring over time.

Long-term bond strength may also be influenced by the internal stresses developed within the joint as a result of brick growth (in clay brickwork) and mortar shrinkage (Baker 1979; Abrams 1995). There are four possible types of shrinkage in a mortar system: plastic shrinkage that occurs before the mortar has set, autogenous shrinkage that occurs as hydration (i.e., curing) takes place, drying shrinkage caused by the partial dehydration of the cement gel, and carbonation shrinkage due to the carbonation of $Ca(OH)_2$ and cement hydration products. The volume changes associated with drying shrinkage are in part reversible but not fully recoverable (Neville and Brooks 1987). Carbonation shrinkage is irreversible and occurs over extended periods of time (Kamimura et al. 1965).

Baker (1979) investigated the effect of ageing on masonry bond strength from 1 to 28 d for various mortars with two types of clay masonry units. Baker found significant "up and down" strength variations and concluded that no clear relationship existed between flexural bond strength and age. Baker suggested that the development of flexural bond strength in masonry may be limited by the poor degree of hydration and (or) shrinkage cracking in the outer portion of mortar joints because of early drying out effects and the possible carbonation of lime that contributes to strength gain.

Matthys and Grimm (1979) investigated the rate of flexural bond strength development, from 8 h up to 28 d, to establish bracing guidelines for lateral wind loads during construction. These authors found a consistent strength gain of up to 3 or 5 d followed by an "up and down" period with a general increase in overall strength. The observed variations in strength were, in some cases, in the order of 40%–50% with the frequency of the variations reducing with age. Drysdale and Gazzola (1985) also investigated the influence of age on bond strength using a limited number of ages: 2, 28, 90 (in some cases), and 365 d. Using *t* test analysis, Drysdale and Gazzola showed that there was no significant difference between 2 and 28 d strength (at 90% confidence limit) and a significant improvement (at a 99.9% confidence level) between 28 and 365 d. From the data presented by Drysdale and Gazzola, it is evident that bond strength also showed an "up and down" behaviour during the 365 d period.

Sise et al. (1988) investigated the influence of age on flexural bond strength from 3 to 365 d for concrete and clay masonry units cured under laboratory conditions with Portland cement – lime (1:1:6) (cement:lime:sand, by volume) and masonry cement (1:3) (cement:sand, by volume) mortars. The results indicated that for the Portland cement – lime mortar, bond strengths after 7 d continued to increase, remained stable, or showed a minor decrease and then stabilized. In contrast, all the results using masonry cement mortars showed a continuous decrease after 7 d with close-to-zero strength remaining after 365 d.

De Vitis et al. (1998) also investigated the influence of age with the purpose of comparing the 7 d bond strength to the strength at other ages. Bond wrench tests were carried out from 1 h to 180 d for two types of clay units using a 1:1:6 mortar and for concrete and calcium silicate units with a 1:0:5 plus water thickener (methyl cellulose) mortar. The results indicated that during the initial 24 h period, the development of bond strength for the methyl cellulose mortar was slower than that for the Portland cement – lime mortar. Following this period, both mortars showed similar steady strength gains up to 7 d with generally 70%–100% of the 7 d strength being reached after only 3 d. Beyond 7 d, while an overall strength gain resulted, an "up and down" behaviour in the order of 30%–40% strength variations was observed. Strength reductions occurred at 14 or 28 d and 180 d, although no set pattern could be identified. De Vitis et al. concluded that despite these variations, the long-term strengths were greater than those exhibited at 7 d and used by the AS3700 standard. De Vitis concluded that further testing extending beyond 180 d with a wider range of materials was needed.

Reda and Shrive (2000) reported on the influence of fly ash addition on flexural bond strength and investigated the mortar microstructure using scanning electron microscopy. Fly ash was used to replace, in part, the Portland cement and lime components in a 1:1:6 mortar and in a 1:0:3 masonry cement mortar. Masonry prisms were constructed and tested for flexural bond strength at 28 d using a bond wrench. A selection of mortars was also tested at ages of 90 and 180 d to investigate the influence of pozzolanic reactions on bond strength. An improvement in bond strength was observed for both mortar types with the addition of fly ash. For the 1:1:6 mortar, the 20% replacement of the lime and Portland cement components resulted in a significant increase in the 28 d flexural strength. Further increases in strength were also observed at 90 and 180 d. Strength gains were noted for the fly ash – masonry cement mortar as well, although these were not as pronounced. Scanning electron microscope (SEM) studies showed the presence of ettringite, calcium hydroxide crystals, unreacted fly ash particles, and calcium silicate hydrate (CSH) gel at the interface. Smaller quantities of calcium hydroxide crystals were also observed with the moist-cured samples. The number of unreacted fly ash particles decreased with longer curing periods. Mortars with high proportions of fly ash showed considerable amounts of microcracking, especially with the dry cured samples.

With the exception of the work by Reda and Shrive (2000), most of this research has been focused on establishing trends rather than investigating the causes of these variations. In a previous study, Lawrence and Cao (1987) compared the 7 d old mortar microstructure to that of a four-year-old wall and found little difference in the degree of hydration between the two samples. The main microconstituents were type I CSH products, ettringite, $Ca(OH)_2$ crystals, and numerous partially hydrated cement particles.

This paper attempts to identify the strength gain and loss mechanisms by correlating the tensile bond strength to the macro and microconstituents formed within the mortar. Bond strengths have been measured at ages ranging from 3–365 d using a small scale direct tension test. The resultant bond strengths were analysed using single factor analysis of variance (ANOVA) and *t* tests to evaluate if the observed differences were statistically significant. Examination of fracture surfaces from the tension specimens, together with polished sections, were carried out using optical and SEM techniques. In addition, X-ray diffraction was employed to

identify the major mortar constituents. These observations were then used to postulate a series of competing mechanisms that may govern masonry bond strength and would need to be confirmed by further experimentation.

Experimental procedure

The bond strength–microstructure relationship was studied at ages of 3, 7, 28, 90, 180, and 365 d. The mortar used was 1:1:6 in combination with a dry pressed clay masonry unit. The initial rate of absorption, cold water absorption, and 5 h boil absorption of the units were determined in accordance with standard AS/NZS4456 (Standards Australia 1997) to be 3.4 kg/m^2 per min, 9%, and 12%, respectively. Brickwork couplets were constructed from a single batch of mortar consisting of 11.2% (by weight) type GP cement, 4.8% bagged hydrated lime, and 84% sand. A local dune sand was used in the investigation. The sand grading is given in Table 1. The fresh mortar properties of flow, cone penetration, and gravimetric air content were determined in accordance with standard AS2701 (Standards Australia 1984) to be 180%, 65% and 3.5%, respectively. The initial water to cement (w/c) ratio (as mixed) of the mortar was 1.90. After construction, the brickwork couplets were covered in plastic for 7 d and then cured in air under laboratory conditions until tested.

At the appropriate age, four couplets were randomly selected and five 25 mm diameter cores were taken along the centreline of each couplet as indicated in Fig. 1. The sampling location, along the couplet centreline, was selected to reduce any edge effects in the outer regions of the bed joint. The loss of bonded area around the perimeter of the joint has been previously identified by van der Pluijm (1996) and Vermeltfoort (2005) as areas where bond is reduced due to poor contact and mortar shrinkage after construction. Coring was carried out using a custom-made, thin-walled, diamond-impregnated coring drill bit with water being used to provide cooling. Once cored, each specimen was trimmed lengthwise to give a 3:1 aspect ratio to help ensure uniform stress distribution during tensile testing. After drying, threaded endplates incorporating double-ended ball joints were glued to each end of the specimen. Details of the tensile test arrangement are shown in Fig. 2.

The specimens were dried and tested as soon as possible after coring, with the time period between coring and testing being approximately 3 d. Testing was carried out using an Instron universal testing machine (model 6027) with a 2 kN pressure transducer load cell. A controlled cross-head displacement of 0.5 mm/min was used. The maximum tensile load and mode of failure was recorded for each specimen. After testing, the fractured specimens were placed in a desiccator for storage until examination. For each age, 10 to 15 specimens were tested. Additional specimens were used as a source for polished or fractured sections.

After failure, the fracture surfaces of the tensile specimens were studied optically and using an SEM. Mortar samples along the top and bottom interfaces were also taken and crushed immediately to a fine powder in a mortar and pestle for X-ray diffraction (XRD). These powders were stored in small airtight containers in a desiccator to minimize carbonation. Powder XRD patterns were obtained using a Philips PW1710 X-ray diffractometer fitted with a cobalt radiation (Cu kα) tube. Scans were carried out in the 2θ range from 2° to 60° using a step size of 0.020° and a 1 s duration. Secondary electron images (SEI) were obtained using a JEOL-840 scanning electron microscope. Samples were gold coated prior to inspection. The nomenclature for the morphology of the CSH products used in this paper is that described by Diamond (1976).

Table 1. Particle size distribution of dune sand.

	Sieve size					
	2.36 mm	1.18 mm	600 μm	300 μm	150 μm	75 μm
% passing	100	100	96	25	1	0

Results

Uniaxial tests and modes of failure

The bond strengths and modes of failure of individual specimens are presented in Table 2. The data shows that strength variations occurred over the testing period. Within each age group and also within each couplet there is a large scatter of data from one couplet to another, indicating that there are local variations in bond strength across the joint. Standard deviations range from 0.20 to 0.47. The normalized strength relative to the 7 d value indicates that the magnitude of strength changes over time, with the 3, 7, and 90 d strengths being similar. Relative to the 7 d mean strength, an average strength gain of 29% was achieved at 28 d with the maximum strength occurring at 180 d (a 32% increase). A large decrease in strength was observed between 28 and 90 d, (with the 90 d strength being only 8% higher than that after 7 d). A smaller decrease was also observed between 180 and 365 d. Despite these fluctuations, the 365 d strength was approximately 20% greater, on average, than the 7 d value. Note that because of the large sampling interval used at the latter ages, it is not possible to ascertain the exact age of the maxima or minima.

Each bond strength data point is plotted in Fig. 3 together with the mean strengths at each age. Again, note the high variation for each age group. A natural logarithmic function has been fitted to the data and this shows that there is a net overall increase in bond strength with time, but with a poor linear correlation. The spread of the data within each age group does not provide a clear pattern of the variation in strength over time, although it tends to indicate that the relationship is not linear, with strength fluctuations occurring over the one year period.

Statistical analysis

An ANOVA analysis was performed on the 3–365 d bond strengths using a 95% confidence limit. The results of the analysis are presented in Table 3 and indicate that age has a significant influence on bond strength (P-value = 5.35×10^{-6}). To evaluate if the observed strength gains and losses with age are statistically significant, t tests were carried out between each sequential age group. A summary of the results and the likelihood of the observation being significant, us-

Fig. 1 View of the drilling machine, thin-walled diamond-tipped core drill bit, and specimen.

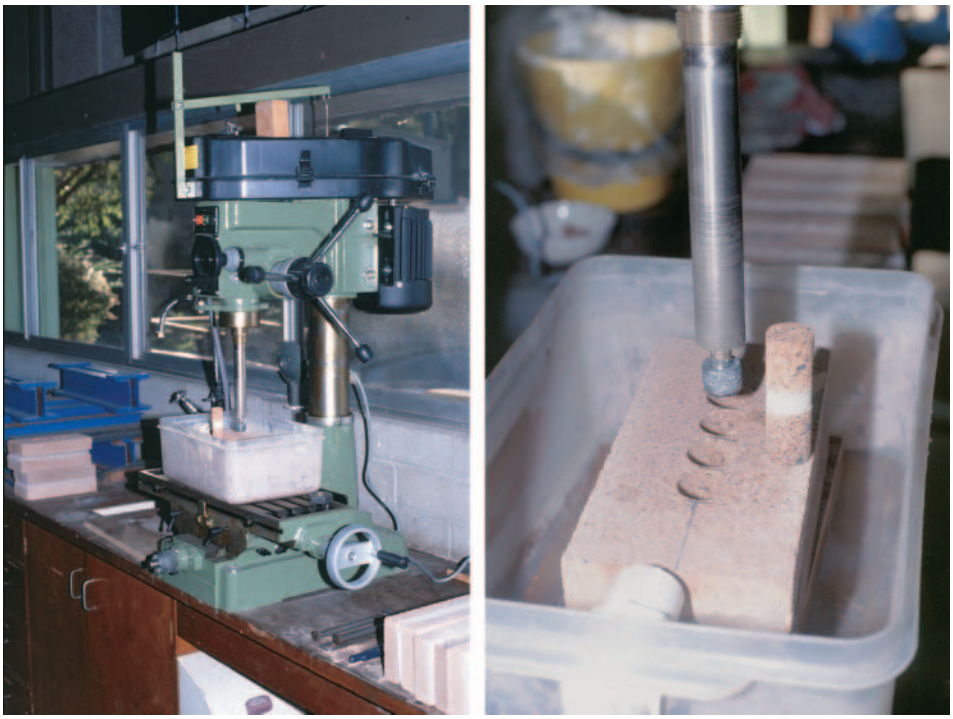

Fig. 2 Details of small-scale uniaxial tension specimens.

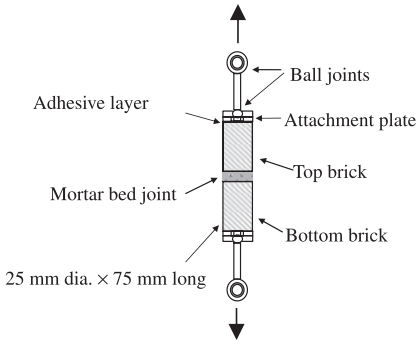

ing a 95% confidence limit, are presented in Table 4. It can be observed that the increase in strength between 7 and 28, and 90, and 180 d are significant while the loss in strength, observed between 90 and 180, and 180 and 365 d have only shown marginal significance. The *t* tests were also performed relative to the 7 d strength and this showed that there were significant increases at 28, 180, and 365 d.

Modes of failure

The common mode of failure was primarily cohesive within the mortar, either at the centre of the mortar joint or 2–3 mm away from the interface. Approximately 20% of all failures were mixed mode in nature, with failure occurring both cohesively within the mortar or brick and along the brick–mortar interface. In some cases, the grainy and poorly consolidated nature of the dry pressed brick specimens allowed failure to occur in the unit away from the mortar joint. For these specimens, an epoxy resin was used to impregnate the brick cores to improve the brick cohesive strength prior to retesting. Care was taken to avoid contamination of the zone around the mortar joints and all fracture surfaces were inspected for the presence of epoxy. These specimens are identified in Table 2.

Optical and scanning electron microscope observations

Specimen failure surfaces

At all ages, the examination of the failure surfaces from the direct tension specimens using the optical microscope showed features which were consistent with those associated with good levels of bond. The brick–mortar had developed good contact along the interface. The interface adhesive failures showed good penetration of paste into the texture of the brick bed surface. Examination of the corresponding mortar surface showed that a dense layer of paste had been in contact with the unit bed surface with some small entrapped air voids (<1 mm diameter). The mortar cohesive failures showed a well-developed coating of paste around the aggregate particles forming bridges of paste linking them together. Fresh aggregate fracture surfaces were also visible, even for the 3 d old samples, implying that adequate paste–aggregate bond had been achieved. Voids of 1–2 mm diameter resulting from entrapped air within the mortar could also be observed.

Evolution of the paste microstructure

The microstructure of the mortar paste was examined under the SEM. Samples were prepared by fracturing the additional cores described earlier. Secondary electron micrographs for the six ages are shown in Fig. 4. It is important to note that variations in the density of the products were observed to occur within each sample. Most likely, these differences arise from different packing densities of the

Table 2. Direct tension test results.

3 d		7 d		28 d		90 d		180 d		365 d	
Direct tension (MPa)	Failure mode	Direct tension (MPa)	Failure mode	Direct tension (MPa)	Failure mode	Direct tension (MPa)	Failure mode	Direct tension (MPa)	Failure mode	Direct tension (MPa)	Failure mode
1.69	MC,TI	1.82	MC, CJ	2.76	MC,TI	1.18	IA, V	2.60	MC,TI	2.16	MC, TI
1.69	MC,TI	1.86	MC, CJ	2.60	IA and BC, BI*	1.46	IA and MC, BI	2.28	MC,TI	1.51	BC, BI
1.97	MC,TI	1.72	MC, CJ	2.38	MC,TI	2.02	MC, TI	2.42	MC, TI	2.44	BC, TI
						2.16	MC, TI*				
						1.79	BC, TI*				
2.09	IA and MC, TI	1.73	MC, CJ	2.06	MC,TI	1.74	MC, BI	2.66	MC, TI	2.13	MC, CJ
		1.70	MC, TI	1.81	IA and MC, BI*	2.08	MC, CJ	2.24	MC, TI	2.01	BC and MC, BI
		1.44	MC, CJ	2.76	IA and MC, BI*	1.99	IA and MC, BI	2.53	MC, TI	2.00	MC, TI
				2.41	IA and MC, BI*	1.63	IA and MC, BI	1.66	BC, BI*	2.09	MC, CJ
										2.18	MC, CJ
1.81	MC,TI	2.00	MC, CJ	2.29	MC, BI	1.95	MC,TI	2.33	MC, CJ	2.48	MC, TI
1.53	MC,TI	1.78	MC, CJ	2.00	IA and MC, BI*	1.66	MC, CJ	2.02	MC,TI	1.99	MC, CJ
1.63	MC,TI	1.47	MC,TI	2.15	MC, CJ	2.34	MC,TI	2.28	MC,TI	2.15	MC, CJ
1.70	MC,CJ	1.32	IA BI, V	0.97	IA and MC, BI*			2.18	MC, CJ	2.14	MC, CJ
1.73	MC, CJ			1.91	MC, CJ			2.27	MC, CJ		
1.72	MC,TI	1.87	MC, CJ	2.26	MC,TI			2.24	MC, BI	1.56	IA, BI
1.48	MC, CJ	1.57	MC, TI					1.81	MC,TI	1.94	IA and BC, BI
1.15	IA,BI							1.93	MC, CJ*	1.75	MC, CJ
Mean = 1.68, SD = 0.24		Mean = 1.69, SD = 0.20		Mean = 2.18, SD = 0.47		Mean = 1.83, SD = 0.32		Mean = 2.23, SD = 0.28		Mean = 2.04, SD = 0.27	
1.00†		1.00†		1.29†		1.08†		1.32†		1.20†	

Note: All values within each cell were obtained from the same couplet. SD, standard deviation; MC, mortar cohesive failure; BC, brick cohesive failure; IA, interface adhesive failure; BI, bottom interface; TI. top interface; CJ, centre of joint; V, void.

*Epoxy-coated brick core.

†Normalized strength (MPa) relative to 7 d value.

Fig. 3 Distribution of tensile bond strengths as a function of age.

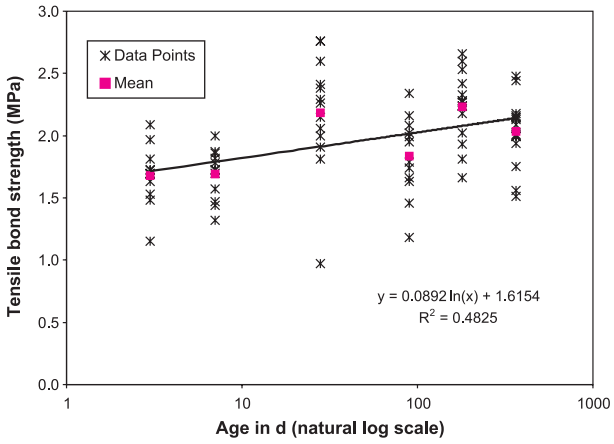

cement particles caused by localized variations in capillary suction. The micrographs shown in Fig. 4 were selected to be as representative as possible.

At a lower level of magnification a general increase in the density of the paste can be observed with time. This gradual change is shown more clearly at the higher magnification shown in Fig. 4. For the 3 d sample, Fig. 4*a*, the CSH structure can be observed to consist of fluffy type I products and some reticular type II products. Note that the discrete boundary between the partly hydrated grains can still be observed. Some $Ca(OH)_2$ crystals were also present, as well as some long fibrous crystals, probably ettringite.

The 7 d sample, shown in Fig. 4*b*, indicates that the CSH products have grown sufficiently to begin to form a network, although the discrete boundary of the particles can still be observed in some regions. Further densification occurred between the 7 and 28 d sample, Fig. 4*c*, with a dense matrix being formed throughout the field of view. In some regions, $Ca(OH)_2$ deposits could also be distinguished, engulfing the CSH structure, and resembling the type IV CSH products. Note that the individual fluffy products of each cement particle did not appear to be as prominent as in the 28 d sample. Another feature that could be observed in the 28 d sample was the appearance of numerous dense reaction rims of CSH products, resembling Hadley's grains. These are most likely associated with the hydration of the dicalcium silicate (C_2S) or of the larger and, therefore, less reactive tricalcium silicate (C_3S) particles.

The samples at 90, 180, and 365 d, Figs. 4*d–f*, respectively, showed type IV CSH structures similar to the 28 d sample with a minor increase in density of the matrix. The formation of dense rim layers around the larger voids may be from carbonation due to the ingress of atmospheric CO_2.

X-ray diffraction studies

X-ray diffraction patterns were carried out on mortar samples for the six ages. The patterns were analysed and the *d*-spacing for the observed phases are summarized in Table 5. The quartz peaks originating from the sand aggregate are numerous and well defined as a result of the high relative proportion of sand in the mortar (84% by weight). The much lower proportions of cement and lime in the mortar and the poor crystallinity of CSH hydration products resulted in low peak intensities for the phases of interest. This made tracing the consumption of the clinker phases and the evolution of CSH, $Ca(OH)_2$, and $CaCO_3$ difficult.

The 3 d sample was the only sample to show some weak intensity peaks from unreacted C_3S implying that most of the C_3S had reacted within 7 d. Note that there is some overlap in the *d*-spacing observed for C_3S, with the intensities at 2.81 Å (1 Å = 0.1 nm) and 3.06 Å being complemented by the CSH and $CaCO_3$ phases.

Portlandite ($Ca(OH)_2$) was present in all patterns. The majority of this phase may be attributed to the lime addition in the mortar. Calcite ($CaCO_3$) was also present in all patterns with a significant increase in peak intensity occurring in the 365 d sample. There is also a possibility that CSH ($Ca_{1.5}SiO_3.xH2O$) was present in the samples. However, this CSH compound has only three reflections, all of which overlapped with peaks from other phases.

Discussion

For the clay masonry unit – 1:1:6 mortar combination studied, an overall net increase in bond strength was observed in the 365 d period of the experiment. Despite the large scatter shown by the bond strength data, the ANOVA and *t* test indicate that during this period there are strength gains and losses. These results exhibit "up and down" behaviours similar to those reported previously, with gain in strength being observed between 3 and 28 d followed by a decrease towards 90 d. Maximum strength was observed at 180 d, with a small decrease as the specimens approached 365 d. Again, note that because of the large sampling interval used at the latter ages, it is not possible to ascertain the exact age of the maxima or minima. The data can only be used as an indication of the changes that have occurred.

This strength–age behaviour was similar to that described by De Vitis et al. (1998), who performed tests using similar raw materials and in the same laboratory. The position of the strength maxima and minima are not consistent across all other published work, indicating that the bond strength–age behaviour is influenced by variations in raw material and environmental conditions. However, the significant increase in strength shown by the statistical analysis at 28, 180, and 365 d relative to the 7 d strength, indicate that there is an overall gain in strength with age. These findings are also consistent with those reported previously by Drysdale and Gazzola (1985) and Reda and Shrive (2000). For this brick–mortar combination, the strength gain with age above that of the 7 d value, as specified in AS3700 (Standards Australia 2001) for the design of masonry structures, will increase the safety margin against out-of-plane loads.

The SEM examination of the mortar allowed the identification of the microconstituents to be type I, II, and IV CSH products, $Ca(OH)_2$, and ettringite. These findings are consistent with the work of Marusin (1983), Chase (1984), and Lawrence and Cao (1987). The SEM study indicated that the maturing of the CSH structure paralleled the strength gain between 3 and 28 d. Beyond 28 d, no further changes could be observed using this technique. This increase in the level of hydration is expected, but is different from that noted by Lawrence and Cao (1987) who observed little differences between a 7 d old paste and 4-year-old mortar. This is likely to reflect the favourable moisture conditions

Table 3. Analysis of variance (ANOVA) for 3–365 d bond strengths.

Summary						
Groups	Count	Sum	Average	Variance		
3 d	12	20.19	1.683	0.0563		
7 d	12	20.28	1.690	0.0407		
28 d	13	28.36	2.182	0.2235		
90 d	12	22.00	1.833	0.1041		
180 d	15	33.45	2.230	0.0788		
365 d	15	30.53	2.035	0.0736		
ANOVA α = 0.05						
Source of variation	SS	df	MS	F	P-value	F_{crit}
Between groups	3.80805	5	0.76161	7.91151	5.3×10^{-6}	2.34003
Within groups	7.02743	73	0.09627	—	—	—
Total	10.8355	78	—	—	—	—

Note: SS, sum of squares; df, degrees of freedom; MS, mean squares; F, variance ratio; F_{crit}, critical F-ratio.

Table 4. Comparison of strength trends between age groups using t tests.

	Age groups				
	3 and 7 d	7 and 28 d	28 and 90 d	90 and 180 d	180 and 365 d
Strength increase or decrease	No change	Increase	Decrease	Increase	Decrease
$P(T \leq t)$ two-tail, α = 0.05	0.934	0.003	0.042	0.003	0.064
Significance level	Not significant	Significant	Marginally significant	Significant	Marginally significant

in these samples, allowing hydration to continue. The XRD allowed the identification of the primary products in the mortar: quartz (sand aggregate), $Ca(OH)_2$, $CaCO_3$, and CSH. The masking by the numerous quartz peaks, the low relative intensities, and the poor crystallinity of the phases of interest reduced the usefulness of XRD to qualitatively monitor the changes in the proportions of phases. However, XRD showed that the majority of C_3S was consumed before 7 d. No clear indication was given for the consumption of C_2S. The XRD also showed that the proportion of $Ca(OH)_2$ decreased at 365 d, with a corresponding increase in the $CaCO_3$ content. No differences could be observed via SEM or XRD for the 90 d sample to account for the 20% loss in strength.

The causes for the strength gain and strength loss behaviour at the latter ages are not apparent from the results of this investigation. It is likely that the observed bond strength is the result of a combination of competing mechanisms as suggested by Baker (1979) — hydration of CSH and carbonation of $Ca(OH)_2$ contributing to strength gains, with (drying) shrinkage and carbonation of CSH phases resulting in volume changes and microcracking being responsible for reductions in strength. By superimposing these mechanisms, it is possible to hypothetically explain the observed bond strength fluctuations with time as indicated in Fig. 5.

The bulk of the initial strength gain at early ages comes from the hydration of the C_3S as indicated by the SEM and XRD observations. Provided adequate moisture is available, hydration of a large portion of C_2S will occur within the 28 d period, with minor quantities of the slower reacting particles continuing to hydrate over a longer time span. Strength losses are likely to be a result of the CSH products undergoing drying shrinkage. Drying shrinkage is, in part, reversible and is likely to contribute to the "saw tooth" behaviour observed by several researchers.

Carbonation has also been reported as a potential source of shrinkage in Portland cement mortars (Kamimura et al. 1965). The increased amount of carbonation between 180 and 365 d may also be an indication that drying of the mortar has occurred, since the carbonation rate increases as the relative humidity within the paste approaches 50% (Cather 1994). The type of aggregate may also contribute to shrinkage, although in this case the sand used in the 1:1:6 mortar had no fine material.

Observations of shrinkage microcracks would require a different experimental approach as the vacuum necessary for conventional SEM work causes shrinkage (dehydration) and cracking to occur. Techniques to measure the pore volume changes that occur as drying shrinkage takes place, such as gas adsorption and (or) desorption, are available but do not readily lend themselves to masonry samples. Recent development of alternating current impedance spectroscopy (ACIS) to Portland cement systems show promising results and further work using this technique on masonry samples is being undertaken (Christensen et al. 1994).

A different approach has been applied successfully in mortars used for concrete repair work where strength losses due to shrinkage have been observed (Banthia and Yan 2000). For these materials, fibres have been incorporated into the mortar or concrete repair material to limit shrinkage and increase the fracture toughness of the mortar. However, the presence of fibres in the fresh mortar is likely to reduce the workability and impede the mason from achieving a uniform bond.

It is also important to note that for this brick–mortar combination, the bond strengths were high and, despite vari-

Fig. 4 Mortar fracture sections obtained at different ages: (*a*) 3 d, (*b*) 7 d, (*c*) 28 d, (*d*) 90 d, (*e*) 180 d, and (*f*) 365 d. Secondary electron image (SEI), bar length = 10 μm.

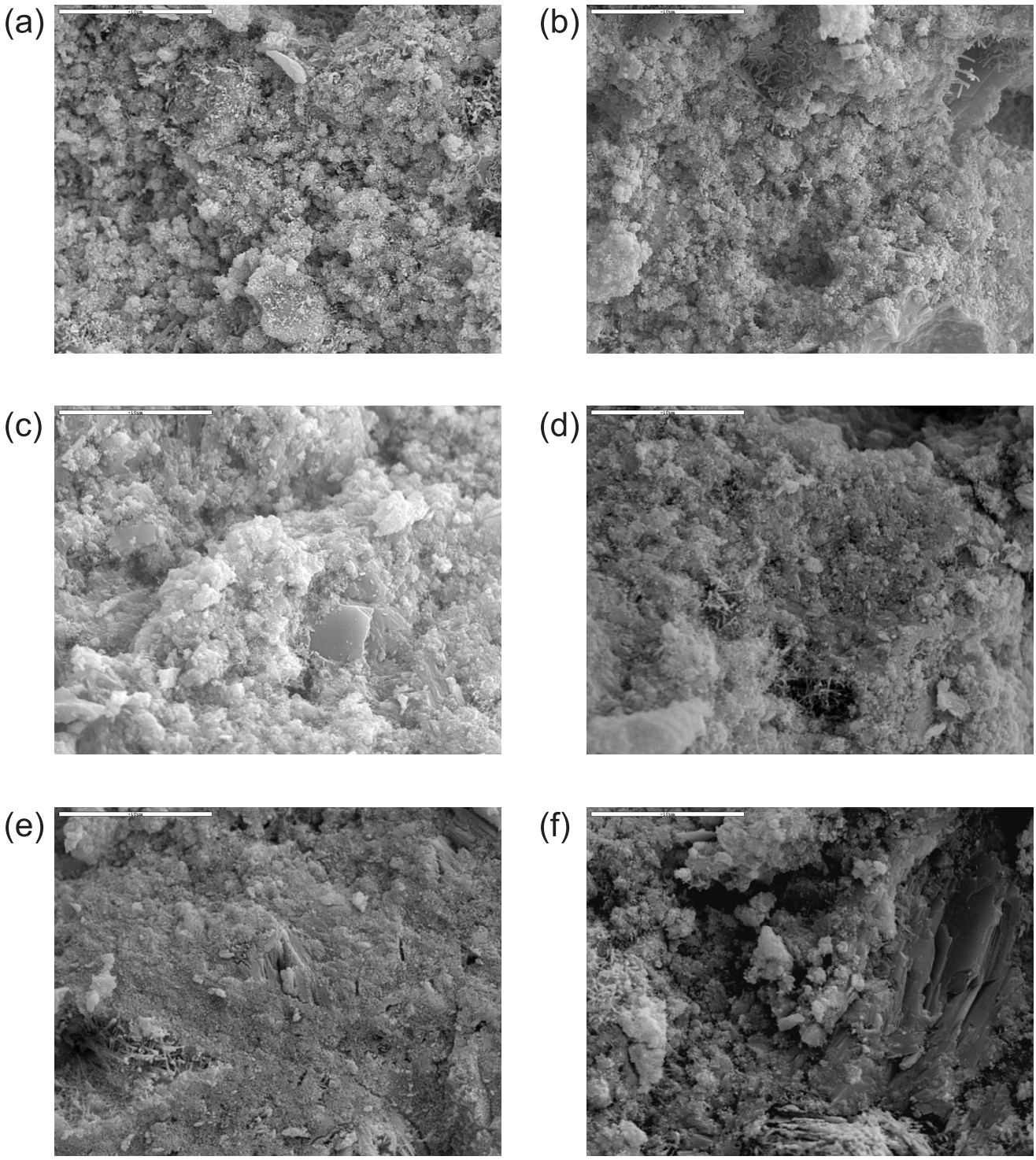

ations in strength, at no stage fell below the 7 d value specified by the Australian masonry standard (Standards Australia 2001) (and used in design). The majority of the modes of failure from the uniaxial tension tests also indicated that these were, in reality, measurements of mortar cohesive strength rather than the bond (interfacial) strength. In some cases, noted in Table 2, the mortar cohesive and bond strengths exceeded the cohesive strength of the masonry unit, requiring the specimens to be retested after impregnating them with epoxy resin.

The influence of age on bond appears to be a complex interaction of mechanisms leading to strength gains and losses and cannot be entirely explained in terms of microstructural changes observed with the SEM. Additional studies incorporating different characterization techniques or the modification of the fracture toughness of the cementitious

Table 5. Summary of phases in mortar obtained from X-ray diffraction patterns.

Phases	*d*-spacing (Å) (1 Å = 0.1 nm) and peak intensity (in decreasing order)*
Quartz (low)	3.35(s), 4.27(s), 2.46(s), 1.82(s) (doublet), 2.29(s), 2.13(s), 2.24(s), 4.27(s), 1.98(s), 1.67(m) (doublet), 1.66(m)
C_3S (3 d sample only)	2.81°(w), 2.20 (w), 2.76(w), 3.06(w), 1.781(w)
$Ca(OH)_2$	2.64(m), 4.96(m), 1.94(m), 1.80(w), 3.12(w)
CSH	3.06(w), 2.81(w), 1.82(w)
$CaCO_3$	3.06(w), 2.29(w), 2.10(w) intensities of peaks increasing in the 365 d sample
Unidentified (90 d sample only)	1.72(w)

*s, strong; m, medium; and w, weak intensities.

Fig. 5 Schematic representation of time-dependent processes affecting bond strength.

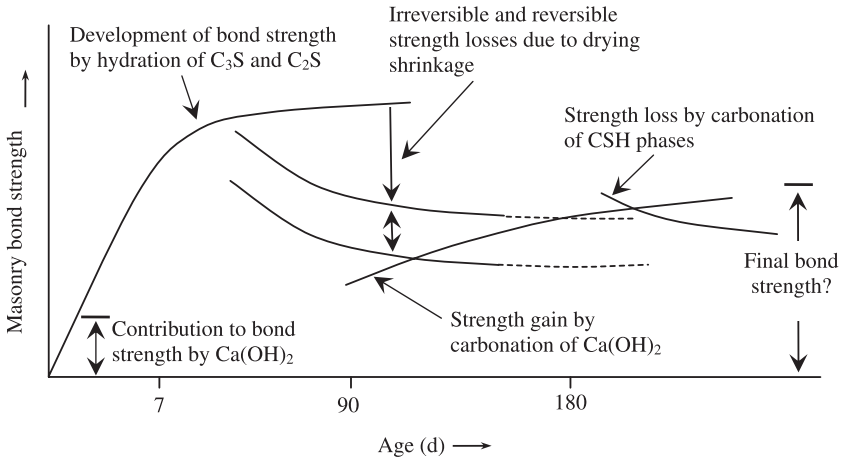

binder phases are required to develop a further understanding of the factors influencing long-term bond strength.

Conclusion

This study investigated the bond strength–microstructure relationship over a 1 year period for a 1:1:6 mortar in combination with a dry pressed masonry unit. The initial improvements in bond strength after 7 d were accompanied by the maturing of the CSH paste structure. Maximum bond strength was observed to occur at 180 d. However, strength losses at 90 and 365 d were also observed. The reasons for these changes in strength were not apparent from this investigation, with only minor differences in the hydration products being observed over this time period. Possible strength reductions may be a result of shrinkage drying and (or) carbonation shrinkage and changes in the fracture toughness of the cementitious paste, associated with loss of moisture from the mortar. A postulate for these competing mechanisms has been proposed. Additional research is required to investigate the influence of these parameters on masonry bond strength.

Acknowledgements

The authors would like to thank the Australian Research Council for their financial support under an Austrailian Research Council (ARC) Discovery Project. The authors would also like to thank Think Brick Australia, and Cement, Concrete and Aggregates Australia (CCAA) for donating materials used in this research.

References

Abrams, D.P. 1995. Effect of mortar shrinkage on in-plane stresses in clay brickwork. TMS Journal, **13**: 77–84.

Baker, L.R. 1979. Some factors affecting the bond strength of brickwork. *In* Proceedings of the 5th International Brick Masonry Conference, Washington, D.C., 5–10 October 1979. The Brick Institute of America, Reston, Va. pp. 84–89.

Banthia, N., and Yan, C. 2000. High-performance fiber reinforced concrete in infrastructural repair and retrofit. *Edited by* N. Krstulovic-Opara and Z. Bayasi. ACI SP 185. American Concrete Institute, Farmington, Mich.

Cather, R. 1994. Curing: The true story? Magazine of Concrete Research, **46**: 157–161.

Chase, G.W. 1984. Investigation of the interface between brick and mortar. TMS Journal, **3**: T1–T9.

Christensen, B.J., Tate Coverdale, R., Olsen, R.A., Ford, S.J., Garbozi, E.J., Jennings, H.M., and Mason, T.O. 1994. Impedance spectroscopy of hydrating cement-based materials: Measurement, interpretation and application. Journal of the American Ceramic Society, **77**(11): 2789–2804. doi:10.1111/j.1151-2916.1994.tb04507.x.

De Vitis, N., Page, A.W., and Lawrence, S.J. 1998. Influence of age on masonry bond strength – A preliminary study. Masonry International, **12**: 64–68.

Diamond, S. 1976. Structure of cement paste. *In* Hydraulic cement pastes: their structure and properties. Proceeding of a Confer-

ence held at Tapton Hall, University of Sheffield, Sheffield, UK, 8–9 April 1976. Cement and Concrete Association, UK.

Drysdale, R.G., and Gazzola, E.A. 1985. Influence of mortar properties on the tensile bond strength of brick masonry. *In* Proceedings of the 7th International Brick Masonry Conference, Melbourne, Australia, 17–20 February 1985. Brick Development Research Institute and University of Melbourne, Melbourne, Australia. pp. 927–938.

Kamimura, K., Serada, P.J., and Swenson, E.G. 1965. Changes in weight and dimensions in the drying and carbonation of Portland cement mortars. Magazine of Concrete Research, **17**: 5–14.

Lawrence, S.J., and Cao, H.T. 1987. An experimental study of the interface between brick and mortar. *In* Proceedings of the 4th North American Masonry Conference, Los Angeles, Calif., 16–19 August 1987. The Masonry Society, Boulder, Colo. Paper 48, pp. 1–14.

Marusin, S.L. 1983. Investigation of the shale brick cement-lime mortar bond using scanning electron microscope (SEM). *In* Proceedings of the 5th International Conference on Cement Microscopy, Nashville, Tenn., 14–17 March 1983. International Cement Microscopy Association, Duncanville, Tex. pp. 180–188.

Matthys, J.H., and Grimm, C.T. 1979. Flexural strength of nonreinforced brick masonry with age. *In* Proceedings of the 5th International Brick Masonry Conference, Washington, D.C., 5–10 October 1979. The Brick Institute of America, Reston, Virg. pp. 114–121.

Neville, A.M., and Brooks, J.J. 1987. Concrete technology. Longman Scientific & Technical, Harlow, UK.

Reda Taha, M.M., and Shrive, N.G. 2000. Enhancing masonry bond using fly ash. Masonry International, **14**: 9–17.

Sise, A., Shrive, N.G., and Jessop, E.L. 1988. Flexural bond strength of masonry stack prisms. *In* Proceedings of the British Masonry Society. No. 2, pp. 103–107.

Standards Australia. 1984. Method of sampling and testing mortar for masonry construction. Standard AS 2701–1984. Sydney, Australia.

Standards Australia. 1997. Masonry units and segmental pavers-methods of test. Standard AS/NZS 4456:1997. Sydney, Australia.

Standards Australia. 2001. Masonry structures. Standard AS 3700–2001. Sydney, Australia.

Sugo, H.O. 2000. Strength and microstructural characteristics of brick/mortar bond. Ph.D. thesis, The University of Newcastle, Newcastle, Australia.

Sugo, H.O., Page, A.W., and Lawrence, S.J. 1997. Characterization and bond strengths of mortars with clay masonry units. *In* Proceedings of the 11th International Brick/Block Masonry Conference (IB^2MAC), Shanghai, China, 14–16 October 1997. Tongji University, Shanghai, China. pp. 59–68.

van der Pluijm, R. 1996. Measuring of bond – A comparative experimental research. *In* Proceedings of the 7th North American Masonry Conference, South Bend, Ind., 2–5 June 1996. University of Notre Dame, South Bend, Ind. pp. 267–281.

Vermeltfoort, A. 2005. Brick–mortar interaction in masonry under compression. Ph.D. thesis, Eindhoven University of Technology, University Press, Eindhoven, the Netherlands.